















Title	Psychiatric-onset neuronal intranuclear inclusion disease in a psychiatry-based dementia-enriched cohort in Japan
Author(s)	Miyamoto, Tesshin; Mori, Kohji; Akamine, Shoshin et al.
Citation	Psychiatry and Clinical Neurosciences. 2025
Version Type	VoR
URL	https://hdl.handle.net/11094/102240
rights	© 2025 The Author(s). Psychiatry and Clinical Neurosciences published by John Wiley & Sons Australia, Ltd on behalf of Japanese Society of Psychiatry and Neurology.
Note	

The University of Osaka Institutional Knowledge Archive : OUKA

<https://ir.library.osaka-u.ac.jp/>

The University of Osaka

Psychiatric-onset neuronal intranuclear inclusion disease in a psychiatry-based dementia-enriched cohort in Japan

Tesshin Miyamoto, MD ¹, Kohji Mori, MD, PhD ^{1,*}, Shoshin Akamine, MD, PhD ¹, Shizuko Kondo, AA,¹ Shiho Gotoh, PhD ¹, Ryota Uozumi, MMSc ¹, Sumiyo Umeda, MD, PhD ¹, Hanako Koguchi-Yoshioka, MD, PhD ², Satoshi Nojima, MD, PhD ³, Daiki Taomoto, MD, PhD ¹, Yuto Satake, MD, PhD ^{1,4}, Takashi Suehiro, MD, PhD,¹ Hideki Kanemoto, MD, PhD ^{1,5}, Kenji Yoshiyama, MD, PhD,¹ Takashi Morihara, MD, PhD ¹ and Manabu Ikeda, MD, PhD¹

Aim: A GGC repeat expansion in the 5' untranslated region of *NOTCH2NLC* is a genetic cause of Neuronal Intranuclear Inclusion Disease (NIID) that exhibits cognitive, motor, and autonomic dysfunction. Our objective is to determine whether there are undiagnosed NIID cases in a psychiatry-based dementia-enriched cohort and to identify their clinical characteristics.

Methods: A retrospective clinical cohort study was conducted in an inpatient and outpatient psychiatric clinic in a University Hospital in Osaka, Japan. Genomic DNA and clinical information were collected with written informed consent. Nine hundred fifty-eight cases were clinically classified according to the International Classification of Diseases (ICD)-10 system. Genetic analysis with Repeat-Primed PCR and Amplicon-Length PCRs were performed.

Results: Of the 958 cases, three were confirmed to have an aberrant GGC repeat expansion in *NOTCH2NLC*. Cases 1 and 2 had preceding anxiety and depressive episodes, and one of these cases also had a mild cognitive impairment.

Case 3 met the diagnostic criteria for progressive supranuclear palsy. All three cases lacked hyperintensity at the corticomedullary border on diffusion-weighted MRI, which is known as a characteristic for NIID. Interestingly, one case exhibited the corticomedullary hyperintensity later in the disease course with apparent neurocognitive decline. All three cases exhibited a mix of slow waves in electroencephalogram and elevated total protein level in cerebrospinal fluid.

Conclusions: NIID is a rare cause of cognitive dysfunction in a psychiatry-based dementia-enriched cohort in Japan. Our data implicates psychiatric symptoms can be prodromal or early manifestation of a subset of NIID cases, thereby extending its phenotypic spectrum.

Keywords: neurodegenerative disease, Neuronal Intranuclear Inclusion Disease, *NOTCH2NLC*, repeat disease, repeat primed PCR.

<http://onlinelibrary.wiley.com/doi/10.1111/pcn.13854/full>

The significance of psychiatric symptoms occurring in the prodromal or early stages of neurodegenerative diseases is increasingly recognized, as seen in the recently proposed research criteria for dementia with Lewy bodies.¹ There is a group of neurodegenerative diseases caused by aberrant expansion of repetitive sequences in a genetic region, such as Huntington's disease, myotonic dystrophy type 1, and *C9orf72*-frontotemporal dementia (FTD)/amyotrophic lateral sclerosis (ALS). Psychiatric symptoms often precede motor and behavioral symptoms, at least in a subset of patients with these repeat expansion disorders.^{2–6} Neuronal intranuclear inclusion disease (NIID) is also a progressive neurodegenerative disease characterized by intranuclear inclusions found in various types of cells throughout the body, including neurons.⁷ An aberrant GGC repeat expansion in the 5' untranslated region (UTR) of the *NOTCH2NLC* gene was identified as a genetic cause of NIID.^{8,9} The *NOTCH2NLC* gene, located on chromosome 1q21.1, is one of the paralogous *NOTCH2NL*-like genes that emerged due to partial duplication of the *NOTCH2* gene.

NOTCH2NLC is stably expressed in radial glia throughout cortical development, and *NOTCH2NL* proteins are postulated to enhance Notch signaling by interacting with Notch receptors, thereby promoting cortical neurogenesis.^{10,11} The common manifestations of NIID are encephalitis-like paroxysmal symptoms, autonomic dysfunction, coordination disorders, cognitive impairment, and muscle weakness.^{7,12} Pathogenic alleles in *NOTCH2NLC* are relatively common in East Asians¹³ and most NIID cases are reported from East Asia,¹⁴ although rare cases have also been reported from Western countries.¹⁵ Hyperintensity at the corticomedullary border on brain MRI has been recognized as a characteristic feature indicative of NIID.¹² However, it should be noted that these imaging findings have only been observed in a proportion of cases of NIID.^{16,17} Apart from neuroimaging findings, intranuclear inclusion bodies can also be found on the skin cells, including sweat gland duct cells, fibroblasts, and fat cells in patients with NIID; therefore, a skin biopsy is useful for the clinical diagnosis of NIID.^{18,19} However, further differential diagnosis

¹ Department of Psychiatry, Graduate School of Medicine, The University of Osaka, Osaka, Japan

² Department of Neurocutaneous Medicine, Division of Health Science, Graduate School of Medicine, The University of Osaka, Osaka, Japan

³ Department of Pathology, Graduate School of Medicine, The University of Osaka, Osaka, Japan

⁴ Division of Psychiatry, University College London, London, UK

⁵ Health and Counseling Center, The University of Osaka, Toyonaka, Japan

* Correspondence: Email: kmori@psy.med.osaka-u.ac.jp

with the other repeat expansion disorders that present intranuclear inclusion pathology in skin tissue, including fragile X-associated tremor/ataxia syndrome (FXTAS), may be required.²⁰ When classifying *NOTCH2NLC* GGC repeat length, it is common to define 61 or more repeats as a pathological expansion, 41–60 as intermediate expansion, and 40 or fewer as non-expansion.^{21,22} While expanded GGC repeat causes NIID, a small number of cases with intermediate GGC repeat expansion have been found in patients with Parkinson's disease,²¹ Alzheimer's disease (AD),²³ ALS,²⁴ and essential tremor (ET).²⁵

The pathophysiology of how the GGC repeat expansion in the *NOTCH2NLC* gene causes neurodegeneration is still largely unexplored. In 2021, it was shown that the pathological GGC repeat expansion is translated into poly-glycine protein, and the poly-glycine protein constitutes the intranuclear inclusions.²⁶ Since then, potential disease mechanisms, including inhibition of nucleocytoplasmic transport,²⁷ RNA toxicity,^{28,29} altered DNA methylation,^{30–32} mitochondrial dysfunction,³³ translational dysfunction,³⁴ and inhibition of ribosome biogenesis³⁵ have been proposed using multiple disease models expressing the GGC repeats.

Because NIID is not yet widely recognized and its clinical phenotype is diverse, patients may be misdiagnosed with other neurodegenerative diseases^{22,23,36–38} or even psychiatric disorders.

Our department (Department of Psychiatry, Graduate School of Medicine, The University of Osaka) has established a mixed cohort of 958 cases of neurodegenerative diseases and psychiatric disorders consisting of Japanese patients. Here, we investigated whether cases of NIID are present in our cohort and, if so, what their clinical characteristics are.

Methods

Patient consent and participants

The protocol for the research project has been approved by suitably constituted Ethics Committees of Osaka University (453-3) and Osaka University Hospital (18470), and conform to the provisions of the Declaration of Helsinki. Participants were recruited from the inpatient ward and outpatient clinic of the Department of Psychiatry, Osaka University Hospital, between April 2015 and January 2025, based on written informed consent. Genomic DNA from peripheral blood leukocytes was obtained from the cases. Demographic information was collected from electronic medical records. All cases were classified in F0 (F00–F09: organic, including symptomatic, mental disorders), F1 (F10–F19: psychoactive substance use), F2 (F20–F29: schizophrenia and the related disorders), F3 (F30–F39: depression and bipolar disorder), F4 (F40–F49: anxiety and related disorder), F5 (F50–F59: behavioral syndromes associated with physical factors), F6 (F60–F69: personality disorders), F7 (F70–F79: intellectual disabilities), F8 (F80–F89: disorders of psychological development), F9 (F90–F98: behavioral and emotional disorders in childhood and adolescence), and G40 category (epilepsy) according to the International Classification of Diseases (ICD-10).³⁹ Cases classified as 'organic, including symptomatic, mental disorders' (F0 group) were further subclassified by clinical diagnosis based on the established diagnostic criteria.^{40–43}

Polymerase chain reaction assays for determination the *NOTCH2NLC* 5' UTR GGC repeat size

Repeat-primed polymerase chain reaction (RP-PCR) was conducted to detect the length of GGC repeat expansions in the *NOTCH2NLC* gene. A fluorescein (FAM)-labeled *NOTCH2NLC*-RP-F primer (5'-GGCATTTGCGCCTGTGCTTCGGACCGT-3'), M13-(GGC)₄(GGA)₂-R primer (5'-CAGGAAACAGCTATGACCTCCTCCGCCGCCGCCGCC-3'), and M13-linker-R primer (5'-CAGGAAACAGCTATGACCG-3') were utilized for RP-PCR.⁹ In cases with 61 or more *NOTCH2NLC* GGC repeats, the repeat lengths were further validated by fluorescence amplicon length polymerase chain reaction (AL-PCR). A FAM-labeled *NOTCH2NLC*-AL-F primer

(5'-CATTTGCGCCTGTGCTTCGGAC-3') and *NOTCH2NLC*-AL-R primer (5'-AGAGCGGCGCAGGGCGGGCATCTT-3') were used for AL-PCR.⁹ The PCR mix contained 0.25 U PrimeSTAR GXL DNA Polymerase, 1× PrimeSTAR GXL Buffer, 0.2mM each of dATP, dTTP, dCTP (Takara Bio), and 7-Deaza-2'-deoxy-guanosine-5'-triphosphate (Roche), 5% dimethyl sulfoxide (Nacalai Tesque), 1 M betaine (Fujifilm-Wako), 0.3 μM each primer mix and 100 ng genomic DNA in both RP-PCR and AL-PCR. Both PCRs were performed using a SimpliAmp™ Thermal Cycler (Applied Biosystems). After incubation at 98 °C for 10 min (min), the cycling conditions were as follows: 16 cycles of 98 °C for 30 s, 66 °C for 1 min with a reduction of 0.5 °C per cycle, and 68 °C for 8 min, and 29 cycles of 98 °C for 30 s (sec), 58 °C for 1 min and 68 °C for 8 min, followed by a final elongation step of 68 °C for 10 min. The ramp rate of all cycling steps was adjusted to 0.6 °C per sec.⁹ Electrophoresis was performed on a 3730xl DNA Analyzer (Thermo Fisher Scientific), and the data were analyzed using Peak Scanner software (Thermo Fisher Scientific). As size standards, GS600LIZ was used for RP-PCR, and 1200LIZ was used for AL-PCR. The repeat length was estimated by counting the peak number of the 3 base pairs saw-tooth tail pattern with RP-PCR. In cases with pathological expansions, the amplicon length of the highest signal peak of the expanded allele was used to estimate the length of the repeat expansion with AL-PCR.⁹

Skin biopsy

Skin biopsies were performed with the patient's consent for the diagnosis of NIID. Skin tissue samples, taken from 10 cm above the lateral malleolus,⁴⁴ were fixed in a 10% formalin solution.

Immunohistochemistry staining

For immunohistochemistry, skin tissues were deparaffinized for 20 min in xylene and dehydrated as follows: ethanol 100% (10 min), ethanol 90%, ethanol 70%, and rinsed in water. Antigen retrieval was performed in a pressure cooker with 10 mM Tris pH 9.0, 1 mM EDTA for 20 min at 120°C. Endogenous peroxidase activity was blocked, and blocking 20 min with 2.5% horse serum and immunostaining was performed overnight at 4°C using anti-p62 antibody (Abcam ab56416, 1/1000) or anti-phosphorylated α-Synuclein antibody, pSyn#64 (Fujifilm Wako 015-25191, 1/2000). Antigen-antibody complexes were visualized by incubation with DAB substrate (MP-7800, Vector Laboratories), and the slides were counterstained with hematoxylin to visualize the nuclei. Images were acquired using a BX51 polarized light microscope (Olympus) and processed with DP-BSW Viewer software (Olympus).

Immunofluorescence staining

Immunofluorescence staining was performed as described previously⁴⁵ with minor modifications. Skin tissues were deparaffinized for 20 min in xylene and dehydrated as follows: ethanol 100% (10 min), ethanol 90%, ethanol 70%, and rinsed in water. Antigen retrieval was performed in a pressure cooker with 10 mM Tris pH 9.0, 1 mM EDTA for 20 min at 120°C. Blocking was performed with 2% fetal calf serum and immunostaining was performed overnight at 4°C using p62 antibody (MBL PM045, 1/1000). Antigen-antibody complexes were visualized by anti-rabbit antibody (Invitrogen A21429, 1/500). After incubation for 20 min with 1.5 μg/mL 4',6-diamidino-2-phenylindole di-lactate (DAPI) to visualize the nuclei, the tissues were incubated with Sudan black solution (0.2% Sudan black B in 70% ethanol/PBS) for 1 min. Images were acquired using a FLUOVIEW FV3000 confocal microscope (Olympus) and processed using FV31S-SW Viewer software (Olympus).

Case selection for subgroup analysis in non-expanded repeat cases

Cases with relatively long repeats (21–40) and corresponding short repeats (≤9) were selected from the non-expanded cases (≤40

repeats). Cases with pathological repeat expansion or missing MRI data were excluded from both groups.

Semi-quantification of white matter hyperintensities in brain MRI

The Fazekas (Fz) scoring system⁴⁶ was used to semi-quantitatively evaluate white matter hyperintensities. The Fz score of each case was evaluated in two regions: periventricular (PV) and deep white matter (DWM) on a scale from 0 to 3, respectively. Moreover, the sum of these scores was calculated as the combined Fz score.

Statistical analysis

Statistical analyses were performed using JMP 17.1.0 (SAS Institute). Comparisons of *NOTCH2NLC* GGC repeat length between ICD-10 classifications or clinical diagnoses were performed using the Kruskal–Wallis test. Comparisons of the age at brain MRI between the two groups with different *NOTCH2NLC* GGC repeat lengths were performed using Welch's *t*-test, and comparisons of Fz scores were performed using Pearson's chi-square test. All quantification data were presented as mean (standard deviation [SD]). A *P*-value of <0.05 was considered statistically significant.

Results

Identification of three cases with pathological *NOTCH2NLC* GGC repeat expansions in a psychiatry-based dementia-enriched cohort

A total of 958 serial cases (535 female and 423 male) were recruited. RP-PCR screening of all cases identified three cases with pathogenic GGC repeat expansions (>60) in the *NOTCH2NLC* 5' UTR. Subsequent AL-PCR analysis confirmed that the estimated number of repeats in the expanded alleles were 186, 118 and 112, respectively. At the initial diagnosis, one case was diagnosed with an anxiety disorder (F4) and another with depression. The latter was subsequently diagnosed with dementia with Lewy bodies (DLB) (F0). The remaining case was diagnosed with progressive supranuclear palsy (PSP) based on MDS clinical diagnostic criteria for PSP.⁴³ Their detailed clinical courses are described in the following section. No cases were classified as belonging to the intermediate group (41 to 60 GGC repeats), and the remaining 955 cases (Table 1, Fig. 1a) were classified as the non-expanded group (40 or less GGC repeats). Of the 955 cases, 820 cases (85.9%) were classified in F0 category (Table 2, Fig. 1b). A bimodal

distribution with peaks at nine repeats and 14 repeats was observed in all cases (Fig. 1c) as well as cases in the F0 category alone (Fig. 1d).

Clinical features of patients harboring GGC repeat expansions in *NOTCH2NLC* 5' UTR

Here we provide a detailed clinical description of the three cases of pathological GGC repeat expansion.

Case 1

Case 1 was a right-handed male patient. His parents divorced when he was 5 years old, and he was subsequently raised by his father and grandfather. He found it difficult to keep up with his learning since he was in elementary school. His father had become unable to eat and exhibited cognitive impairment but was not clinically investigated in detail. His father eventually died at age 57 when the patient was 16 years old. Although he got a job after graduating from high school, his food intake decreased around the same time and he developed an unbalanced diet. He changed job every few years, and by age 27 he lost his job and he began receiving welfare benefits. He led an isolated and sedentary life. At age 30, he became malnourished, with difficulty eating for unknown reasons. He was referred to a psychiatric facility and diagnosed with generalized anxiety disorder. Afterward, his activity level temporarily improved and his motivation to go out increased, and he started going to an employment support facility. At age 34, he developed neurogenic bladder. The following year, he developed cholecystitis and liver dysfunction. In that same year, his grandfather died at age of 92 from symptoms similar to those of his father's. This triggered phobic anxiety disorders, resulting in depressive symptoms accompanied by insomnia and loss of appetite. Although his insomnia improved with lemborexant, he continued to suffer from loss of appetite, and his weight decreased from 80 to 60 kg. At age 36, a brain MRI revealed mild generalized atrophy. His Mini-Mental State Examination (MMSE) score was 26, implicating the presence of mild cognitive impairment, and he was referred to our department for further investigation. When he was admitted to our hospital, tremors localized to his upper extremities, impairment of postural reflexes and short-stepped gait were observed. There was no miosis, rigidity, muscle weakness, or increased or decreased tendon reflexes. Blood tests showed elevated liver enzymes (aspartate aminotransferase [AST] 89 U/L, alanine aminotransferase [ALT] 210 U/L, and gamma-glutamyl transpeptidase [γ -GTP] 272 U/L) hyperbilirubinemia (direct-bilirubin [D-Bil] 2.0 mg/dL, indirect-Bil [I-Bil] 1.1 mg/dL) and

Table 1. Number of cases, age of onset and GGC repeat length per ICD-10 classification in non-expanded cases

ICD-10 code	Disease category	Case	Onset age	<i>N2C</i> 5' UTR GGC repeat length		
				Average	Maximum	Minimum
F0	Organic, including symptomatic mental disorder	820	70.8 (\pm 9.37)	15.4 (\pm 4.63)	35	3
F1	Mental and behavioral disorders due to psychoactive substance use	15	68.7 (\pm 9.18)	15.1 (\pm 3.36)	20	9
F2	Schizophrenia, late onset schizophrenia-like psychosis	43	68.3 (\pm 15.0)	15.1 (\pm 4.98)	32	7
F3	Mood disorders	24	57.1 (\pm 17.1)	15.7 (\pm 6.48)	32	5
F4	Neurotic disorders	18	58.6 (\pm 15.5)	15.3 (\pm 4.79)	28	9
F5	Behavioral disorders associated with psychological disturbances and physical factors	5	71.4 (\pm 4.59)	16.6 (\pm 2.94)	20	13
F6	Adult personality and behavioral disorders	4	64.3 (\pm 9.91)	14.3 (\pm 1.79)	16	12
F7	Mental retardation	1	57.0 (\pm 0.00)	14.0 (\pm 0.00)	14	14
F8	Disorders of psychological development	5	42.2 (\pm 14.9)	12.6 (\pm 2.15)	15	10
F9	Behavioral and emotional disorders with onset usually occurring in childhood and adolescence	5	58.6 (\pm 10.2)	17.8 (\pm 3.71)	24	14
G40	epilepsy	15	60.3 (\pm 14.1)	16.2 (\pm 3.76)	23	9
total		955	69.7 (\pm 10.8)	15.4 (\pm 4.66)	35	3

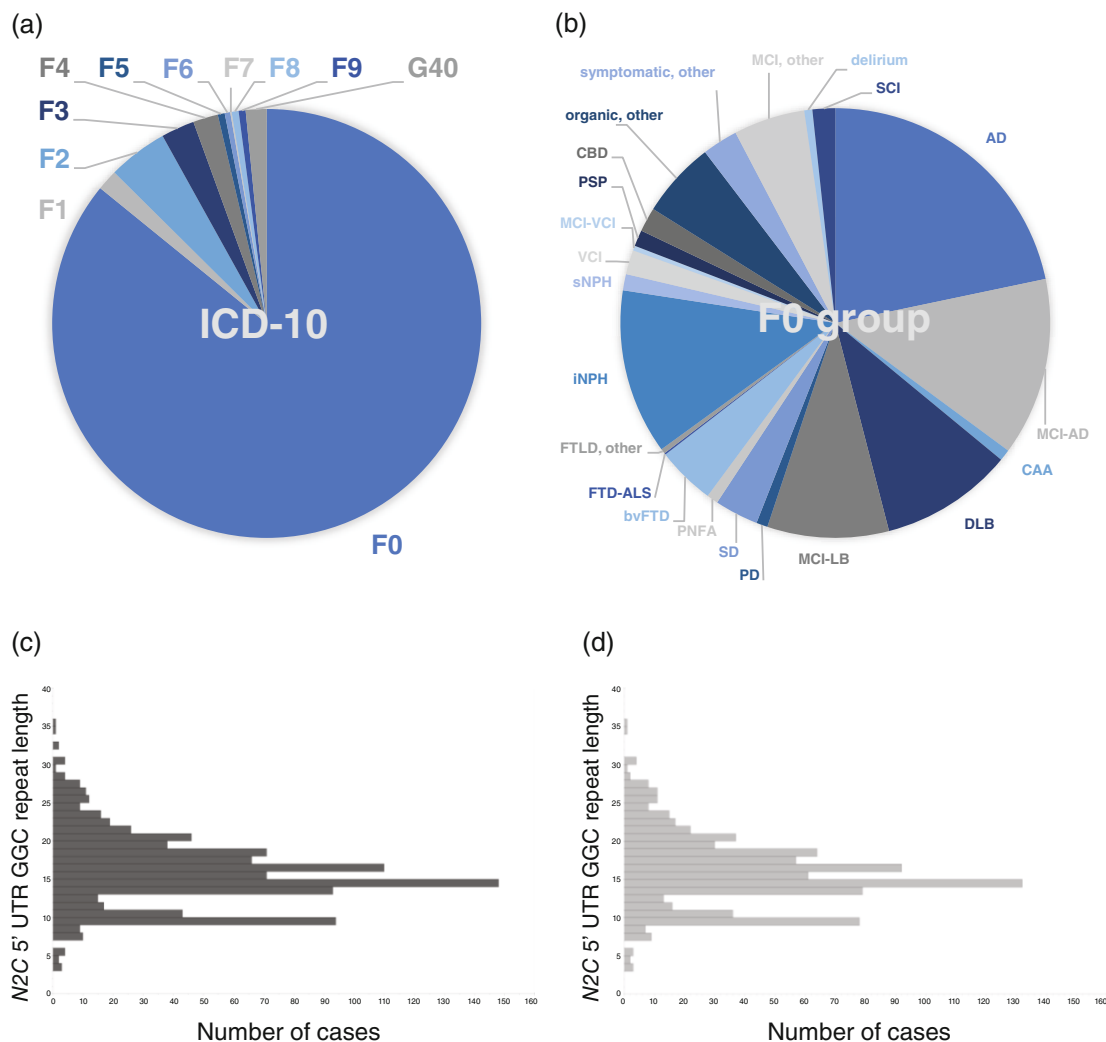


Fig. 1 Distribution of *NOTCH2NLC* GGC repeat lengths in non-expanded cases. (a) The frequency of ICD-10 classification. (b) The frequency of clinical diagnosis in F0 group. (c) A histogram showing repeat length distribution of ICD-10 classification. (d) A histogram showing repeat length distribution of cases classified in F0 group.

pancreatic amylase (P-Amy 139 U/L). These data suggested the presence of biliary system dysfunction even though he seldom drank alcohol. No organic lesion was found in the biliary system on radiological imaging, and these data were gradually improved with an increase in food intake. Blood tests also showed no evidence of diabetes, and no autoantibodies were detected. His cerebrospinal fluid (CSF) examination showed elevated total protein (58 mg/dL) and glucose (82 mg/dL). Tau protein (171 pg/mL) and phosphorylated threonine 181 tau (p-tau) protein (21 pg/mL) in CSF were within the normal range. IgG index was within the normal range. Electroencephalography (EEG) showed a mix of 6–7 Hz slow waves. Brain MRI showed no specific findings other than mild atrophy of the parietal and temporal lobes. Periventricular hyperintensity was observed bilaterally (Fig. 2a for fluid-attenuated inversion recovery (FLAIR) image and 2b for diffusion-weighted image; DWI at age 37). IMP-SPECT revealed decreased perfusion in the parietal lobe, temporal lobe, occipital lobe, precuneus, and cingulate gyrus. Motor nerve conduction velocity (MNCV) in the median nerve was decreased on the left (44.9 m/s) compared to the right (60.5 m/s). MNCV in the ulnar nerve was decreased bilaterally: 46.7 m/s on the right and 47.5 m/s on the left. Sensory nerve conduction velocity (SNCV) revealed no specific findings.

He scored 16 out of 18 on the Frontal Assessment Battery (FAB). Results of the Wechsler Adult Intelligence Scale (WAIS)-IV test showed a full-scale intelligence quotient (FIQ) of 70, indicating

mild intellectual disability. His symptoms did not meet the diagnostic criteria for any type of dementia. Tentative psychiatric diagnosis at his discharge was phobic anxiety disorders, acute stress response due to his grandfather's death, autonomic dysfunction, mild cognitive impairment possibly due to malnutrition, and/or mild intellectual disability. The diagnosis of NIID was made retrospectively by the identification of a *NOTCH2NLC* GGC repeat expansion (>60) in RP-PCR (Fig. 2c). AL-PCR confirmed the expansion of 186 GGC repeats (Fig. 2d). CGG repeat expansion in *FMRI* 5' UTR, CAG repeat expansion in *ataxin-1*, *ataxin-2*, *MJD1*, *CACNA1A*, *TBP* and *atrophin-1*, CTG repeat expansion in *KLH1* and TGGAA repeat expansion in *BEAN/TK1* were ruled out. Skin biopsy confirmed the presence of ubiquitin- and/or p62-positive inclusion bodies in the nuclei of sweat gland duct cells (Fig. 2e,g) and arrector pili muscle cells (Fig. 2f). At age 37, his nutritional status deteriorated again due to loss of appetite, and total parenteral nutrition was temporarily introduced. He developed cholecystitis and underwent a cholecystectomy, after which his appetite improved. At age 38, loss of appetite and constipation recurred. Both of which improved with the administration of sodium picosulfate 7.5 mg/day. The MMSE score at that time was 21, indicating progressive cognitive impairment. Despite the decline in MMSE scores, brain MRI findings were unchanged, with no diffuse hyperintensity area or corticomedullary hyperintensities

Table 2. Number of cases, age of onset and GGC repeat length per clinical diagnostic classification in non-expanded cases of the F0 group

Initial diagnosis of F0 group cases	Case	Onset age	N2C 5' UTR GGC repeat length		
			Average	Maximum	Minimum
AD	178	68.7 (± 10.3)	16.0 (± 4.98)	30	4
MCI-AD	110	71.6 (± 8.50)	14.7 (± 4.55)	27	3
CAA	7	73.7 (± 3.99)	18.0 (± 3.82)	24	13
DLB	82	75.0 (± 7.86)	16.1 (± 5.20)	35	7
MCI-LB	75	72.5 (± 6.97)	16.0 (± 4.62)	27	5
PD	7	57.6 (± 9.88)	15.1 (± 2.90)	19	10
SD	27	65.6 (± 6.98)	14.7 (± 4.02)	26	9
PNFA	7	65.3 (± 8.84)	14.1 (± 3.27)	19	10
bvFTD	36	64.4 (± 9.09)	15.6 (± 4.40)	30	9
FTD/ALS	1	53.0 (± 0.00)	14.0 (± 0.00)	14	14
FTLD, other	3	72.0 (± 3.56)	13.3 (± 2.49)	16	10
PSP	10	68.3 (± 11.8)	15.5 (± 2.58)	19	10
CBD	15	64.3 (± 6.63)	15.7 (± 3.82)	23	9
iNPH	102	74.7 (± 5.58)	14.1 (± 4.23)	26	3
sNPH	10	66.1 (± 12.0)	13.9 (± 4.23)	20	9
VCI	15	71.1 (± 7.94)	17.0 (± 5.42)	29	9
MCI-VCI	3	79.0 (± 4.55)	13.7 (± 0.47)	14	13
organic, other	47	68.3 (± 11.5)	16.5 (± 4.53)	30	9
symptomatic, other	22	69.9 (± 9.20)	16.2 (± 3.61)	24	9
MCI, other	44	74.9 (± 7.60)	14.7 (± 4.35)	25	5
delirium	5	78.0 (± 4.77)	15.2 (± 1.60)	17	13
SCI	14	68.5 (± 10.8)	15.1 (± 4.37)	23	5
total	820	70.8 (± 9.37)	15.4 (± 4.63)	35	3

AD, Alzheimer's disease; bvFTD, behavioral variant frontotemporal dementia; CAA, cerebral amyloid angiopathy; CBD, corticobasal degeneration; DLB, dementia with Lewy bodies; iNPH, idiopathic normal pressure hydrocephalus; MCI, mild cognitive impairment; PD, Parkinson's disease; PNFA, progressive nonfluent aphasia; PSP, progressive supranuclear palsy; SCI, subjective cognitive impairment; SD, semantic dementia; sNPH, secondary NPH; VCI, vascular cognitive impairment.

characteristic of NIID cases (Fig. 2h for FLAIR image and 2i for DWI at age 39).

Case 2

Case 2 was a right-handed female patient. Until age 61, she had no history of consultation with a psychiatric or neurological clinic. There was no family history of dementia. At age 62, she developed depressive symptoms and began visiting a psychiatric facility. Although she was diagnosed with depression and received SSRIs, her symptoms did not improve, and she continued receiving treatment at various hospitals. At age 66, she developed an action tremor that was predominantly affecting her right upper limb, and by age 68, tremor in her left upper limb also became noticeable. Around the same time, she developed a masked face, muscle rigidity in her right lower limb, as well as forgetfulness. Brain MRI revealed global mild brain atrophy with hyperintensity area with no diffuse hyperintensity or corticomedullary hyperintensities characteristic of NIID cases (Fig. 2j for FLAIR image and 2k for DWI). Dopamine transporter SPECT (¹²³I-ioflupane) were performed at age 68 and 70, respectively, but showed no decrease in dopamine transporter uptake in the bilateral striatum. Her Parkinsonian symptoms gradually worsened.

At age 73, she exhibited disorientation to place, and visual hallucinations of a child. She was diagnosed with probable DLB based on progressive cognitive impairment, Parkinsonian symptoms, and recurrent visual hallucinations. By this time, brain MRI revealed atrophy of the frontal and parietal lobes, thinning of the corpus callosum, and hyperintensity area at periventricular region and at deep white matter (Fig. 2l). A linear area of hyperintensity along the corticomedullary

border on diffusion-weighted images emerged (Fig. 2m). She was referred to our hospital for further evaluation. Tremor and mild grasp reflex were observed on the right side. Deep tendon reflexes in lower limbs were decreased bilaterally. There was no miosis, rigidity, muscle weakness, impairment of postural reflexes and gait disturbance. At the time of her admission, her MMSE and FAB scores were 22 and 9, respectively, suggesting cognitive impairment. Her blood tests showed no specific findings. Total protein (87 mg/dL) was elevated in her CSF. Tau protein (450 pg/mL) was within the normal limits, and p-tau protein (66 pg/mL) was slightly elevated. IgG index was within the normal range. EEG revealed no epileptic discharge, but a mixed 6–7 Hz generalized slow waves. MNCV showed no specific findings in the right median nerve (46.8 m/s), and in the right ulnar nerve (56.2 m/s). SNCV revealed no specific findings. IMP-SPECT revealed decreased perfusion in the left parietal lobe, left temporal lobe, bilateral frontal lobes, and anterior cingulate gyrus. The diagnosis of NIID was confirmed because *NOTCH2NLC* GGC repeat expansion (> 60) was identified in RP-PCR. This case was confirmed to have 118 repeats by AL-PCR. CGG repeat expansion in *FMR1* 5' UTR was ruled out. Skin biopsy revealed ubiquitin- and/or p62-positive inclusion bodies in the nuclei of sweat gland duct cells (Fig. 2n,p) and fat cells (Fig. 2o). However, no phosphorylated alpha-synuclein-positive structures were observed (data not shown).

Case 3

Case 3 was a right-handed male patient. After graduating university, he started managing a factory in his 20s and continued thereafter. At the age of 63, he developed memory impairment, struggled with work

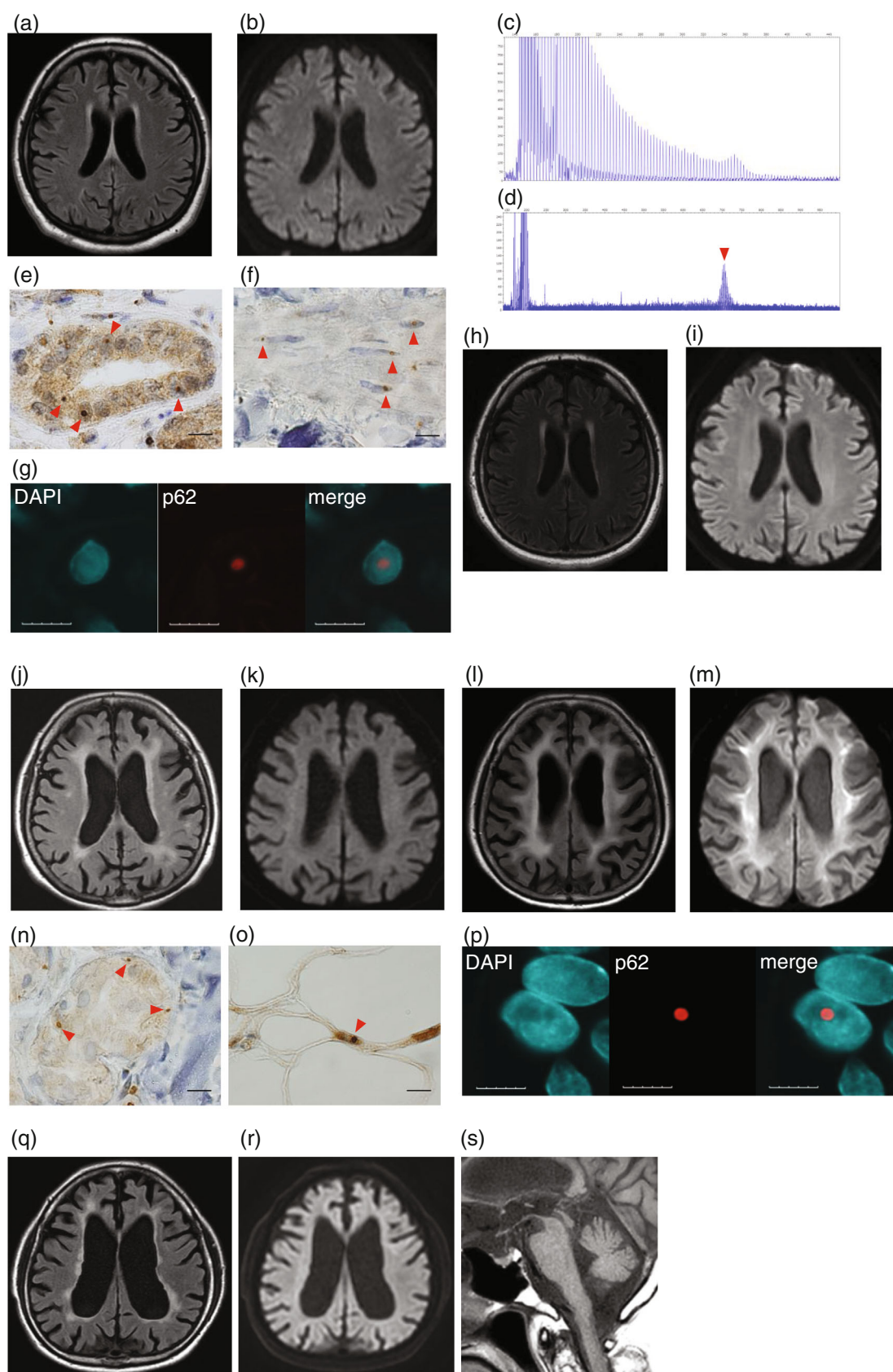


Fig. 2 Legend on next page.

and driving, became restless, laughed inappropriately, showed less interest, and spoke less. After his younger brother's dementia diagnosis, who died suddenly while taking a bath a few years later, he visited a local hospital where a CT scan showed global brain atrophy. He was diagnosed with Alzheimer's disease and began treatment with donepezil. At the age of 65, he showed short-stepped gait. He stopped donepezil, but his short-stepped gait persisted. At the age of 66, he was referred to our hospital. He showed frontal lobe dysfunction, including disinhibited and impulsive behavior, susceptibility to influence, and stereotypic behavior. His MMSE and FAB scores were 18 and 6, respectively. Neurological examination revealed impaired vertical eye movement, short-stepped and freezing of gait, impaired swallowing reflex, action tremor, urinary and fecal incontinence. Despite prominent postural instability, no muscle weakness, no rigidity, and no impairment of postural reflex was observed. No medical record regarding miosis or tendon reflexes were found retrospectively. His blood tests showed no specific findings. In CSF both total protein (64 mg/dL) and total tau (898 pg/mL) were elevated. Aβ1-42/1-40 ratio was 0.095 (threshold 0.0705), ruling out amyloid pathology.⁴⁷ EEG showed background activity at 7–8 Hz, with intermittent 2–4 Hz generalized slow waves, but no epileptic discharge. Brain MRI showed moderate global brain atrophy including midbrain tegmentum and bilateral periventricular hyperintensity (Fig. 2q–s). Two years later, brain MRI confirmed further progression of atrophy in the midbrain tegmentum. The lateral ventricles and third ventricle were enlarged. The Evans Index was 0.37. iNPH was considered as a differential diagnosis, but we did not adopt the diagnosis since there were no tightened sulci in the high convexity or dilatation of the Sylvian fissure. The presence of enlargement of the third ventricle in PSP cases is considered useful in differentiating it from PD.⁴⁸ The ratio derived by dividing the width of the third ventricle (12.19 mm) by the largest internal skull diameter (151.61 mm) was 0.08, which exceeded the cutoff values⁴⁸ consistent with the imaging characteristics of PSP. As for the midbrain atrophy, the anteroposterior diameter of the midbrain was 9.21 mm. The areas of the midbrain and pons in the midsagittal section were 94.60 mm² and 315.74 mm², respectively, yielding a midbrain-to-pons ratio⁴⁹ of 0.30. Both results indicate the presence of midbrain atrophy in this case and were consistent with the diagnosis of PSP. In contrast, hyperintensity at the corticomedullary border, which is indicative of NIID, was absent. IMP-SPECT revealed decreased blood flow in the frontal lobe, cingulate cortex, putamen, parietal lobe, and right medial temporal lobe. Dopamine Transporter SPECT (123I-ioflupane) and MIBG myocardial scintigraphy were normal. The patient was diagnosed with probable PSP. *NOTCH2NLC* GGC repeat expansion (> 60) was retrospectively identified in RP-PCR. This case was confirmed to have 112 repeats by AL-PCR. Skin biopsy and nerve conduction studies were not performed in this case.

No correlation between the non-expanded *NOTCH2NLC* GGC repeat length and diagnostic classification of mental disorders

To examine the potential contribution of the non-expanded repeats to mental disorders in our cohort, we determined how the 955

non-expanded repeat carriers were distributed in terms of ICD-10 classification (Table 1, Fig. 1a). There were no significant differences in *NOTCH2NLC* GGC repeat length among ICD-10 classification groups (F0–F9, G40) ($\chi^2(10) = 6.05$, $P = 0.811$, Fig. 3a). Then we focused on organic mental disorders. Eight hundred and twenty non-expanded repeat carriers, classified into F0 group, were subclassified by the specific clinical diagnosis and plotted for each repeat length (Table 2, Fig. 1b). No significant associations between *NOTCH2NLC* GGC repeat length and each initial clinical diagnosis in the F0 group ($\chi^2(21) = 26.96$, $P = 0.172$, Fig. 3b). Together, the non-expanded repeat was not apparently associated with any diagnosis of neurodegenerative diseases or any other psychiatric disorder in our cohort.

Correlation analysis between white matter hyperintensity and non-expanded *NOTCH2NLC* GGC repeat length

Diffuse white matter lesions detected by T2-weighted or FLAIR of brain MRI is a characteristic feature of NIID cases,^{16,50–54} and pathological expansion of GGC repeats in the *NOTCH2NLC* 5' UTR is one of the causes of adult leukoencephalopathies.⁵⁴ We hypothesized that even cases with non-expanded repeat length (40 or less), those with relatively long repeat lengths might show signs of leukoencephalopathy. To assess the hypothesis, groups with relatively long repeats (21–35, $n = 117$, mean [SD] repeat length = 24.1 [2.98], mean [SD] age of onset = 70.3 [11.0], mean [SD] age at MRI = 74.3 [10.3]) and corresponding short repeats (≤ 9 , $n = 121$, mean [SD] repeat length = 8.40 [1.37], mean [SD] age of onset = 69.8 [11.1], mean [SD] age at MRI = 74.7 [9.4]) were selected from the non-expanded cases (see method, Fig. 4a). There was no significant difference in age of onset ($t(236) = 0.316$, $P = 0.753$) or age at brain MRI ($t(232) = 0.280$, $P = 0.779$) between the two groups. The Fazekas (Fz) scoring system is a semi-quantitative grading score that assesses the severity of periventricular hyperintensity (PVH) and deep white matter hyperintensity (DWMH) and is widely used. Tai *et al.* reported that the Fz score of white matter lesions correlated with MMSE and MoCA scores for cognitive function.⁵⁵ To determine whether there was a correlation between the repeat length and white matter hyperintensity, we assessed the Fz scores for the two groups. Results indicate no significant differences in Fz scores were observed between the two groups for PVH ($\chi^2(3) = 1.78$, $P = 0.619$, Fig. 4b), for DWMH ($\chi^2(3) = 0.738$, $P = 0.864$, Fig. 4c) or for the combined total score ($\chi^2(6) = 3.71$, $P = 0.717$, Fig. 4d). While pathological *NOTCH2NLC* GGC repeat expansion has been linked to white matter hyperintensity and leukoencephalopathy, our results suggest that the difference of repeat length within non-pathological range (≤ 40 repeats) is not associated with abnormal white matter signals on MRI.

Discussion

In the current study, we identified three cases of pathological GGC repeat expansion in *NOTCH2NLC* out of 958 cases of psychiatry-based dementia-enriched clinical cohort. In terms of frequency, we found pathologically expanded *NOTCH2NLC* repeat in 0.31% (3 of 958 cases) in our cohort, which is comparable to previous studies

Fig. 2 Clinical and pathological details of three cases of NIID. (a, b) Brain MR image of case 1 at age 37. (a) T2-weighted fluid-attenuated inversion recovery (T2-FLAIR) image, (b) diffusion weighted image (DWI). Hyperintensity area was observed in periventricular (PV) region and was rated as Fazekas (Fz) score = 1. No findings characteristic of NIID can be identified. (c) Electropherogram of the repeat-primed polymerase chain reaction (RP-PCR) of NIID case 1. (d) Electropherogram of the fluorescence amplicon length polymerase chain reaction (AL-PCR) confirmed 186 GGC repeats in the *NOTCH2NLC* 5' UTR in case 1. (e, f) Immunohistochemical staining of skin tissue in case 1. (e) Ubiquitin-positive inclusion bodies (arrowheads) in the nuclei of sweat gland duct cells. 1000 \times . Scale bar = 10 μ m. (f) p62-positive inclusion bodies (arrowheads) in the nuclei of arrector pili muscle cells. 1000 \times . Scale bar = 10 μ m. (g) Immunofluorescence staining of skin tissue in case 1. A p62-positive inclusion body in the nucleus of sweat gland duct cell. From left to right: DAPI, p62, and merged images. 2000 \times . Scale bar = 5 μ m. (h, i) MR images of case 1 at age 39. (h) T2-FLAIR, (i) DWI. Hyperintensity area was rated as Fz score = 1 at PV region. No findings characteristic of NIID can be identified. (j, k) MRI of case 2. (j) T2-FLAIR at age 66, (k) DWI at age 68. Hyperintensity areas were rated as Fz score = 2 at PV region and 1 at deep white matter (DWM) region. (l, m) MRI of case 2 at age 73. (l) T2-FLAIR, (m) DWI. White matter lesions in T2-FLAIR and hyperintensity at the corticomedullary border in DWI were observed. Hyperintensity areas were rated as Fz score = 3 at both PV and DWM regions. (n, o) Immunohistochemical examination of skin tissue in case 2. (n) p62-positive intranuclear inclusions (arrowheads) in sweat gland duct cells. 1000 \times . Scale bar = 10 μ m. (o) Ubiquitin-positive intranuclear inclusion (arrowhead) in fat cells. 1000 \times . Scale bar = 10 μ m. (p) Immunofluorescence staining of the skin in case 2. A p62-positive inclusion body in the nucleus of sweat gland duct cell. From left to right: DAPI, p62, and merged images. 2000 \times . Scale bar = 5 μ m. (q–s) MRI of case 3 at age 66. (q) T2-FLAIR, (r) DWI, (s) T1 sagittal images. Hyperintensity area was observed rated as Fz score = 3 at PV region.

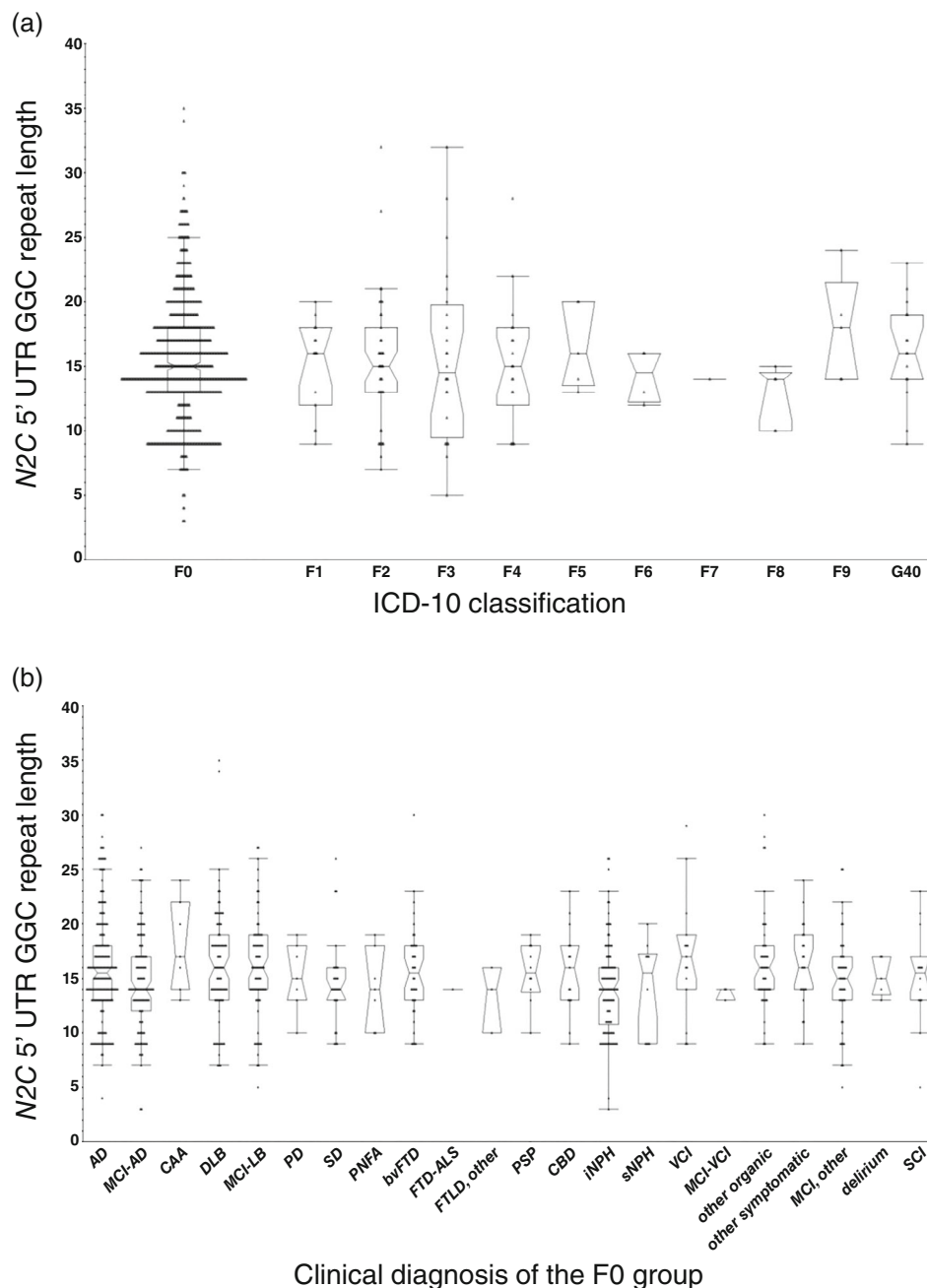


Fig. 3 Distribution of *NOTCH2NLC* GGC repeat lengths for non-expanded cases on ICD-10 classification. (a) Boxplot of *NOTCH2NLC* GGC repeat lengths on each ICD-10 classification. The boxes show the first quartile (1Q), the median, and the third quartile (3Q). The median of each classification is expressed as a notch. The whiskers show the maximum value at the top and the minimum value at the bottom. Values outside the range of $1Q$ or $3Q \pm 1.5 \times IQR$ were defined as outliers. (b) Boxplot of *NOTCH2NLC* GGC repeat lengths on each clinical diagnosis of the F0 group. Alzheimer Disease (AD), mild cognitive impairment (MCI) due to AD, cerebral amyloid angiopathy (CAA), Dementia with Lewy bodies (DLB), MCI due to DLB, Parkinson's disease (PD), semantic dementia (SD), progressive nonfluent aphasia (PNFA), behavioral variant frontotemporal dementia (bvFTD), FTD/ALS, other FTD, progressive supranuclear palsy (PSP), corticobasal degeneration (CBD), idiopathic normal pressure hydrocephalus (iNPH), secondary NPH (sNPH), vascular cognitive impairment (VCI), MCI due to VCI, other organic disorders, other symptomatic disorders, other MCI, delirium, and subjective cognitive impairment (SCI).

from China identifying expanded *NOTCH2NLC* repeat in 0.35% (3 of 861 cases) in Alzheimer's disease²³ and in 0.40% (4 of 1004 cases) in neurodegenerative dementia.³⁶ As in the three cases presented, the frequency was low, and no specific symptoms were identified. Therefore, it has been difficult to diagnose NIID without genetic testing or skin biopsy. Our study is novel in that it examines the *NOTCH2NLC* GGC repeat lengths of various psychiatric disorders included in a psychiatry-based dementia-enriched cohort in Japan. In this study, the repeat length in non-expanded cases was not associated with any

specific ICD-10 classification of psychiatric disorders. This result reinforces the evidence that having no more than 40 GGC repeats in *NOTCH2NLC* 5' UTR is not associated with any specific disease condition, even in the context of a psychiatry-based cohort. Moreover, when compared to short repeat length (≤ 9), relatively longer (but still non-expanded) repeat length ($21 \leq \leq 40$) is not associated with abnormal white matter signals on MRI. This result supports the idea that ≤ 40 *NOTCH2NLC* 5' UTR GGC repeat length is not linked to white matter damage.

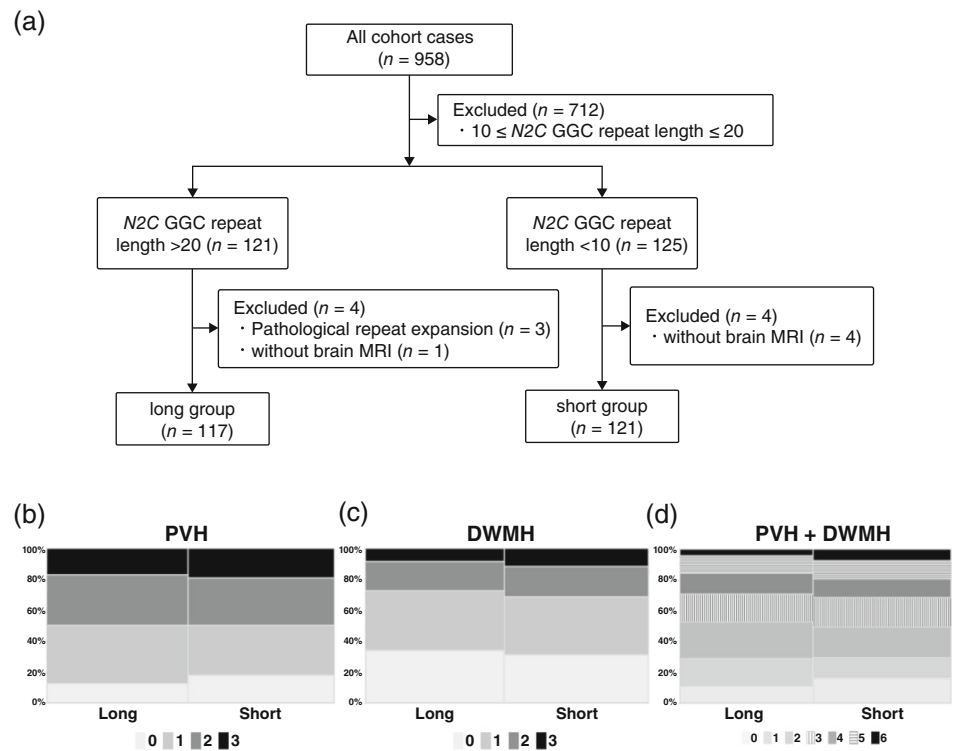


Fig. 4 The Fazekas (Fz) scores for short and long repeat length groups extracted from non-expanded cases. (a) Protocol of case selection. (b–d) Mosaic plots of Fz scores. (b) Periventricular hyperintensity (PVH), (c) Deep white matter hyperintensity (DWMH), (d) Combined Fz score.

It is noteworthy that two out of three NIID cases in our cohort had prior psychiatric diagnoses; case 1 was initially diagnosed with an anxiety disorder, and case 2 was initially diagnosed with depression, followed by a diagnosis of dementia with Lewy bodies. A considerable proportion of patients with NIID may experience significant mood and personality changes, which are often underrecognized.³⁷ A report from the Chinese NIID registry⁵⁵ noted that behavioral and psychiatric symptoms were observed in 31.4% of cases (70 out of 223); however, detailed characterization of these symptoms remains limited. Kawarabayashi *et al.* described a NIID case in which a patient was hospitalized in a psychiatric facility due to delusions and auditory hallucinations that emerged during the disease course.⁵⁶ These cases illustrate that a range of psychiatric and behavioral symptoms can manifest during the course of NIID. Although an incidental co-occurrence cannot be ruled out, the present findings suggest that psychiatric symptoms can be prodromal or early manifestation preceding the emergence of characteristic neurological or radiological findings in a subset of NIID cases. To investigate whether these psychiatric symptoms are prodromal manifestations of NIID, a prospective study involving participants with confirmed *N2C* GGC repeat pathological expansion and familial non-carriers may be useful.

Our initial diagnosis of the third NIID patient was PSP. There is only one case report describing PSP-like presentation of NIID.⁵⁷ Brain MRI findings of the reported case and our third NIID case (probable PSP) were consistent: periventricular white matter hyperintensity, mild ventricular distortion, and midbrain atrophy. They also lacked high intensity signals on diffusion-weighted images.

Elevated liver deviation enzymes such as AST, ALT, and γ -GTP in NIID case 1 could be attributed to biliary dyskinesia that may have been caused by autonomic dysfunction. Indeed, he later developed necrotizing cholecystitis and underwent a cholecystectomy at age 38. The common laboratory findings in our three NIID cases included a mix of slow waves on EEG and elevated total protein in CSF. Increased total protein concentrations in the CSF has been reported in NIID cases presenting with memory impairment,^{58–60} as well as autoimmune encephalitis-like symptoms⁶¹ and episodic headaches.⁶² Based on our NIID cases and these reports, elevated total protein

levels in CSF may be a common finding in NIID.⁶³ To date, there have been no previous reports on EEG findings in NIID. Further case accumulation is needed to determine the extent to which elevated total protein and mixing of slow waves on EEG are common in NIID.

These three cases differed in the presence or absence of characteristic brain MRI findings of NIID, but none of the cases exhibited these findings when psychiatric or neurocognitive symptoms first appeared. This finding may suggest that psychiatric symptoms precede the appearance of brain MRI abnormalities in the disease progression of NIID. Considering that the characteristic brain MRI findings of NIID appear later than the onset of clinical symptoms, diagnosing NIID that begins with psychiatric symptoms might be more difficult, especially in the early stage. Based on these findings, it may be necessary to consider including NIID in the differential diagnosis of progressive cognitive impairment preceded by psychiatric symptoms. In Cases 2 and 3, FAB scores were markedly impaired compared to MMSE scores. Our results are consistent with previous studies that reported the decline in FAB scores was more prominent than that of MMSE scores,^{7,59} implicating early impairment of frontal lobe function in NIID. NIID has been reported to present with a variety of clinical symptoms, including encephalitis-like paroxysmal symptoms, autonomic dysfunction, coordination disorders, cognitive impairment, and muscle weakness. However, no widely accepted diagnostic criteria for clinical diagnosis of NIID have yet been established. Although case selection for advanced testing requires careful consideration, analysis of *NOTCH2NL* 5' UTR GGC repeat length and confirmation of intranuclear inclusions by skin biopsy, are conclusive. In suspected NIID cases, the coexistence of autonomic and motor dysfunction, in addition to cognitive dysfunction, as well as the results of EEG and CSF examination, may be helpful in approaching the diagnosis. However, if NIID-specific findings on brain MRI were included as prerequisite in the diagnostic criteria, the diagnosis of NIID may be delayed.

Although this study showed that NIID cases may develop psychiatric symptoms early on, one limitation is that it is a single facility cohort-based study. It is desirable to conduct research that spans multiple facilities or is conducted on an even larger scale to elucidate the

development of psychiatric symptoms in NIID cases. Future case studies are also needed to characterize psychiatric symptoms in NIID. Collectively, our study demonstrated that NIID is a rare cause of cognitive dysfunction but does exist in a certain percentage in a Japanese psychiatry-based dementia-enriched cohort. Our data suggest that psychiatric symptoms can be prodromal or early manifestation of NIID, thus expanding the diverse phenotypic spectrum of the disease.

Acknowledgments

The authors would like to thank all patients and their families who agreed to participate in this study. This study was supported by Center for Medical Research and Education, Graduate School of Medicine, The University of Osaka. We thank Ms. Mariko Kihara for her assistance in DNA collection. KM is supported by the JSPS KAKENHI grant numbers JP22K19492; JP24K02382, JST FOREST Program under grant number JPMJFR200Z; AMED grant number JP23dk0207066; SENSHIN Medical Research Foundation, The Mochida Memorial Foundation for Medical and Pharmaceutical Research and Takeda Science Foundation. M.I. is supported by AMED grant number JP23bm0804034.

Author contributions

K.M. conceived and Te.M. and K.M. designed the study. Te.M. performed all experiments, analyzed all results and prepared all figures and tables. S.A., S.K., S.G. and R.U. helped with the design of the experiments and analysis of data. H.K.-Y. performed skin biopsies. S.N. stained the skin tissue specimens with ubiquitin antibody and provided neuropathological insights. Ta.M. and S.A. organized the collection of DNA samples. Te.M., K.M., S.U., D.T., Y.S., T.S., H.K., K.Y. and M.I. contributed the collection of clinical information and clinical diagnosis. D.T. and H.K. performed quantification of brain MRI images for the NIID case 3. K.M. and M.I. supervised the research and acquired funding. K.M. wrote the manuscript together with Te.M. All authors discussed the results and approved the final manuscript.

Disclosure statement

The authors declare no competing interests.

Data availability statement

The data are not publicly available due to restrictions on their containing information that could compromise the privacy of research participants. Under these restrictions, the data that support the findings of this study are available on reasonable request to the corresponding author.

References

- McKeith IG, Ferman TJ, Thomas AJ *et al.* Research criteria for the diagnosis of prodromal dementia with Lewy bodies. *Neurology* 2020; **94**: 743–755.
- Snowden JS, Rollinson S, Thompson JC *et al.* Distinct clinical and pathological characteristics of frontotemporal dementia associated with C9ORF72 mutations. *Brain* 2012; **135**: 693–708.
- Kertesz A, Ang LC, Jesso S *et al.* Psychosis and hallucinations in frontotemporal dementia with the C9ORF72 mutation. *Cogn. Behav. Neurol.* 2013; **26**: 146–154.
- van Duijn E, Craufurd D, Hubers AAM *et al.* Neuropsychiatric symptoms in a European Huntington's disease cohort (REGISTRY). *J. Neurol. Neurosurg. Psychiatry* 2014; **85**: 1411.
- Epping EA, Kim J-I, Craufurd D *et al.* Longitudinal psychiatric symptoms in prodromal Huntington's disease: A decade of data. *Am. J. Psychiatry* 2016; **173**: 184–192.
- Mori K, Ikeda M. Biological basis and psychiatric symptoms in frontotemporal dementia. *Psychiatry Clin. Neurosci.* 2022; **76**: 351–360.
- Sone J, Mori K, Inagaki T *et al.* Clinicopathological features of adult-onset neuronal intranuclear inclusion disease. *Brain* 2016; **139**: 3170–3186.
- Ishiura H, Shibata S, Yoshimura J *et al.* Noncoding CGG repeat expansions in neuronal intranuclear inclusion disease, oculopharyngodistal myopathy and an overlapping disease. *Nat. Genet.* 2019; **51**: 1222–1232.
- Sone J, Mitsuhashi S, Fujita A *et al.* Long-read sequencing identifies GGC repeat expansions in NOTCH2NLC associated with neuronal intranuclear inclusion disease. *Nat. Genet.* 2019; **51**: 1215–1221.
- Suzuki IK, Gacquer D, Heurck RV *et al.* Human-specific NOTCH2NLC genes expand cortical neurogenesis through Delta/Notch regulation. *Cell* 2018; **173**: 1370–1384.
- Fiddes IT, Lodewijk GA, Mooring M *et al.* Human-specific NOTCH2NLC genes affect NOTCH signaling and cortical neurogenesis. *Cell* 2018; **173**: 1356–1369.e22.
- Tian Y, Zhou L, Gao J *et al.* Clinical features of NOTCH2NLC-related neuronal intranuclear inclusion disease. *J. Neurol. Neurosurg. Psychiatry* 2022; **93**: 1289–1298.
- Ibañez K, Jadhav B, Zanovello M *et al.* Increased frequency of repeat expansion mutations across different populations. *Nat. Med.* 2024; **30**: 1–12.
- Zhao B, Yang M, Wang Z *et al.* Clinical characteristics of two patients with neuronal intranuclear inclusion disease and literature review. *Front. Neurosci.* 2022; **16**: 1056261.
- Santis TD, Politi LS, Valente EM, Albanese A. MRI abnormalities identify neuronal Intranuclear inclusion disease. *Ann. Neurol.* 2024; **95**: 1009–1010.
- Okubo M, Doi H, Fukui R *et al.* GGC repeat expansion of NOTCH2NLC in adult patients with leukoencephalopathy. *Ann. Neurol.* 2019; **86**: 962–968.
- Wang H, Feng F, Liu J *et al.* Sporadic adult-onset neuronal intranuclear inclusion disease without high-intensity signal on DWI and T2WI: A case report. *BMC Neurol.* 2022; **22**: 150.
- Sone J, Tanaka F, Koike H *et al.* Skin biopsy is useful for the antemortem diagnosis of neuronal intranuclear inclusion disease. *Neurology* 2011; **76**: 1372–1376.
- Sone J, Kitagawa N, Sugawara E *et al.* Neuronal intranuclear inclusion disease cases with leukoencephalopathy diagnosed via skin biopsy. *J. Neurol. Neurosurg. Psychiatry* 2014; **85**: 354.
- Toko M, Ohshita T, Kurashige T *et al.* FXTAS is difficult to differentiate from neuronal intranuclear inclusion disease through skin biopsy: A case report. *BMC Neurol.* 2021; **21**: 396.
- Shi C, Fan Y, Yang J *et al.* NOTCH2NLC intermediate-length repeat expansions are associated with Parkinson disease. *Ann. Neurol.* 2021; **89**: 182–187.
- Huang X-R, Tang B-S, Jin P, Guo J-F. The phenotypes and mechanisms of NOTCH2NLC-related GGC repeat expansion disorders: A comprehensive review. *Mol. Neurobiol.* 2022; **59**: 523–534.
- Wu W, Yu J, Qian X *et al.* Intermediate-length CGG repeat expansion in NOTCH2NLC is associated with pathologically confirmed Alzheimer's disease. *Neurobiol. Aging* 2022; **120**: 189–195.
- Wan M, He J, Huo J, Sun C, Fu Y, Fan D. Intermediate-length GGC repeat expansion in NOTCH2NLC was identified in Chinese patients with amyotrophic lateral sclerosis. *Brain Sci.* 2023; **13**: 85.
- Ng ASL, Lim WK, Xu Z *et al.* NOTCH2NLC GGC repeat expansions are associated with sporadic essential tremor: Variable disease expressivity on long-term follow-up. *Ann. Neurol.* 2020; **88**: 614–618.
- Boivin M, Deng J, Pfister V *et al.* Translation of GGC repeat expansions into a toxic polyglycine protein in NIID defines a novel class of human genetic disorders: The polyG diseases. *Neuron* 2021; **109**: 1825–1835.e5.
- Zhong S, Lian Y, Luo W *et al.* Upstream open reading frame with NOTCH2NLC GGC expansion generates polyglycine aggregates and disrupts nucleocytoplasmic transport: Implications for polyglycine diseases. *Acta Neuropathol.* 2021; **142**: 1003–1023.
- Deng J, Zhou B, Yu J *et al.* Genetic origin of sporadic cases and RNA toxicity in neuronal intranuclear inclusion disease. *J. Med. Genet.* 2022; **59**: 462–469.
- Yu J, Deng J, Guo X *et al.* The GGC repeat expansion in NOTCH2NLC is associated with oculopharyngodistal myopathy type 3. *Brain* 2021; **144**: awab077.
- Fukuda H, Yamaguchi D, Nyquist K *et al.* Father-to-offspring transmission of extremely long NOTCH2NLC repeat expansions with contractions: Genetic and epigenetic profiling with long-read sequencing. *Clin. Epigenetics* 2021; **13**: 204.
- Kameyama S, Mizuguchi T, Doi H *et al.* Patients with biallelic GGC repeat expansions in NOTCH2NLC exhibiting a typical neuronal intranuclear inclusion disease phenotype. *Genomics* 2022; **114**: 110469.
- Cao Y, Tian W, Wu J, Song X, Cao L, Luan X. DNA hypermethylation of NOTCH2NLC in neuronal intranuclear inclusion disease: A case-control study. *J. Neurol.* 2022; **269**: 6049–6057.

33. Yu J, Liufu T, Zheng Y *et al*. CGG repeat expansion in NOTCH2NLC causes mitochondrial dysfunction and progressive neurodegeneration in drosophila model. *Proc. Natl. Acad. Sci.* 2022; **119**: e2208649119.
34. Liu Q, Zhang K, Kang Y *et al*. Expression of expanded GGC repeats within NOTCH2NLC causes behavioral deficits and neurodegeneration in a mouse model of neuronal intranuclear inclusion disease. *Sci. Adv.* 2022; **8**: eadd6391.
35. Fan Y, Li M, Yang J *et al*. GGC repeat expansion in NOTCH2NLC induces dysfunction in ribosome biogenesis and translation. *Brain* 2023; **146**: 3373–3391.
36. Jiao B, Zhou L, Zhou Y *et al*. Identification of expanded repeats in NOTCH2NLC in neurodegenerative dementias. *Neurobiol. Aging* 2020; **89**: 142.e1–142.e7.
37. Liu Y, Li H, Liu X *et al*. Clinical and mechanism advances of neuronal intranuclear inclusion disease. *Front. Aging Neurosci.* 2022; **14**: 934725.
38. Zhang T, Bao L, Chen H. Review of phenotypic heterogeneity of neuronal Intranuclear inclusion disease and NOTCH2NLC-related GGC repeat expansion disorders. *Neurol. Genet.* 2024; **10**: e200132.
39. Brämer GR. International statistical classification of diseases and related health problems. Tenth revision. *World Health Stat. Q* 1988; **41**: 32–36.
40. Rascovsky K, Hodges JR, Knopman D *et al*. Sensitivity of revised diagnostic criteria for the behavioural variant of frontotemporal dementia. *Brain* 2011; **134**: 2456–2477.
41. McKhann GM, Knopman DS, Chertkow H *et al*. The diagnosis of dementia due to Alzheimer's disease: Recommendations from the National Institute on Aging-Alzheimer's Association workgroups on diagnostic guidelines for Alzheimer's disease. *Alzheimers Dement.* 2011; **7**: 263–269.
42. McKeith IG, Boeve BF, Dickson DW *et al*. Diagnosis and management of dementia with Lewy bodies: Fourth consensus report of the DLB consortium. *Neurology* 2017; **89**: 88–100.
43. Höglinger GU, Respondek G, Stamelou M *et al*. Clinical diagnosis of progressive supranuclear palsy: The movement disorder society criteria. *Mov. Disord.* 2017; **32**: 853–864.
44. Itamoto S, Yanagi T, Yabe I, Matsuno Y, Ujiie H. Skin biopsies for diagnosing neuronal intranuclear inclusion disease: A retrospective study of 12 cases. *J. Dermatol.* 2023; **50**: 931–934.
45. Mori K, Nihei Y, Arzberger T *et al*. Reduced hnRNP A3 increases C9orf72 repeat RNA levels and dipeptide-repeat protein deposition. *EMBO Rep.* 2016; **17**: 1314–1325.
46. Fazekas F, Barkhof F, Wahlund LO *et al*. CT and MRI rating of white matter lesions. *Cerebrovasc. Dis.* 2002; **13**: 31–36.
47. Satake Y, Kanemoto H, Gotoh S *et al*. Cerebrospinal fluid amyloid beta with amyloid positron emission tomography concordance rates in a heterogeneous group of patients including late-onset psychotic disorders: A retrospective cross-sectional study. *Psychogeriatrics* 2023; **23**: 1091–1093.
48. Quattrone A, Antonini A, Vaillancourt DE *et al*. A new MRI measure to early differentiate progressive supranuclear palsy from De novo Parkinson's disease in clinical practice: An international study. *Mov. Disord.* 2021; **36**: 681–689.
49. Massey LA, Jäger HR, Paviour DC *et al*. The midbrain to pons ratio. *Neurology* 2013; **80**: 1856–1861.
50. Kutsuna F, Tateishi Y, Yamashita K *et al*. Perfusion abnormality in neuronal intranuclear inclusion disease with stroke-like episode: A case report. *Cereb. Circ. Cogn. Behav.* 2022; **3**: 100127.
51. Yoshii D, Ayaki T, Wada T *et al*. An autopsy case of adult-onset neuronal intranuclear inclusion disease with perivascular preservation in cerebral white matter. *Neuropathology* 2022; **42**: 66–73.
52. Wang Y, Fan Y, Yu W-K *et al*. NOTCH2NLC expanded GGC repeats in patients with cerebral small vessel disease. *Stroke Vasc. Neurol.* 2023; **8**: 161–168.
53. Liao Y-C, Wei C-Y, Chang F-P *et al*. NOTCH2NLC GGC repeat expansion in patients with vascular leukoencephalopathy. *Stroke* 2023; **54**: 1236–1245.
54. Lee G-H, Jung E, Jung N-Y, Mizuguchi T, Matsumoto N, Kim E-J. Case report: Neuronal intranuclear inclusion disease initially mimicking reversible cerebral vasoconstriction syndrome: Serial neuroimaging findings during an 11-year follow-up. *Front. Neurol.* 2024; **15**: 1347646.
55. Tai H, Wang A, Zhang Y *et al*. Clinical features and classification of neuronal Intranuclear inclusion disease. *Neurol. Genet.* 2023; **9**: e200057.
56. Kawarabayashi T, Nakamura T, Seino Y *et al*. Disappearance of MRI imaging signals in a patient with neuronal intranuclear inclusion disease. *J. Neurol. Sci.* 2018; **388**: 1–3.
57. Tian M, Han Y, Bi Y *et al*. Neuronal intranuclear inclusion disease mimicking progressive supranuclear palsy. *Neurol. Sci.* 2023; **44**: 1411–1414.
58. Araki K, Sone J, Fujioka Y *et al*. Memory loss and frontal cognitive dysfunction in a patient with adult-onset neuronal intranuclear inclusion disease. *Intern. Med.* 2015; **55**: 2281–2284.
59. Sugiyama A, Sato N, Kimura Y *et al*. MR imaging features of the cerebellum in adult-onset neuronal intranuclear inclusion disease: 8 cases. *Am. J. Neuroradiol.* 2017; **38**: 2100–2104.
60. Sun L, Zhou L, Ren L, Han C, Xue Q, Ma L. Neuronal intranuclear inclusion disease with subclinical peripheral neuropathy: A case report. *Medicine* 2024; **103**: e40636.
61. Li J, Zhang G, Zheng J, Hu J, Li Y. A case report of neuronal intranuclear inclusion disease and literature review. *BMC Neurol.* 2024; **24**: 488.
62. Shrimpton M, Gasser YP, Sexton A, Malhotra A. Episodic headaches and cognitive decline: Uncovering neuronal intranuclear inclusion disease in a young patient. *BMJ Case Rep.* 2025; **18**: e262351.
63. Kurihara M, Komatsu H, Sengoku R *et al*. CSF P-Tau181 and other biomarkers in patients with neuronal Intranuclear inclusion disease. *Neurology* 2023; **100**: e1009–e1019.